Rigotti, T.; Casado Sánchez, A.; Cabrera, S.; Pérez-Ruiz, R.; Líras, M.; De La Peña-O'shea, V.; Alemán, J. (2018). A Bifunctional Photoaminocatalyst for the Alkylation of Aldehydes: Design, Analysis, and Mechanistic Studies. ACS Catalysis. 8(7):5928-5940. https://doi.org/10.1021/acscatal.8b01331

A Bifunctional Photo-Aminocatalyst for the Alkylation of Aldehydes: Design, Analysis and Mechanistic Studies

Thomas Rigotti,[a] *Antonio Casado-Sánchez,*[a] *Silvia Cabrera,*[b,c] *Raúl Pérez-Ruiz,*[d] *Marta Liras,*[d] *Víctor A. de la Peña O'Shea,*[d] *and José Alemán*[a,c]*

[a] Organic Chemistry Department, Módulo 1, Universidad Autónoma de Madrid, 28049 Madrid (Spain)

[b] Inorganic Chemistry Department, Módulo 7, Universidad Autónoma de Madrid, 28049 Madrid (Spain)

[c] Institute for Advanced Research in Chemical Sciences (IAdChem), Universidad Autónoma de Madrid, 28049 Madrid (Spain).

[d] Photoactivated Processes Unit, IMDEA Energy, Av. Ramón de la Sagra 3, 28935, Móstoles (Madrid, Spain)

KEYWORDS: Bifunctional photocatalyst • Organocatalysis • Pyrrolidines • Photochemistry • Mechanism

ABSTRACT. A new bifunctional photoaminocatalyst based on imidazolidinone and thioxanthone is presented. The preparation of these catalysts proceeds in a two-step synthesis which allows an easy tuning of the steric properties. The photophysical and electrochemical data of the imidazolidinone photocatalysts have been determined, indicating that the catalyst can work under visible light conditions. In order to corroborate the experimental observations, ground state geometry optimization and energy transition studies of thioxanthone and the bifunctional catalyst **4c** were optimized by TD DFT calculations. The alkylation of aldehydes with this amino-photocatalyst works with excellent enantioselectivities and yields due to the stereoelectronic properties of the catalyst. A rational mechanistic cycle based on different mechanistic experiments, TD DFT calculations, and laser flash photolysis is presented.

INTRODUCTION

Photocatalysis has emerged as one of the best strategies for the development of sustainable and novel processes for the synthesis of organic compounds.[1] In spite of the enormous growth in this area, the vast majority of the methodologies developed provide achiral or racemic compounds using either metallic complexes or organic molecules as a photocatalyst. The main reason for this is the difficulty of combining a chiral catalyst to induce a sterochemical control, with the high reactivity and low activation barriers of radical intermediates.[2] In spite of this difficulty, asymmetric photocatalytic transformations have been successfully accomplished by the use of a dual-catalyst approach using a combination of a photocatalyst and a chiral organocatalyst.[3] The use of only one catalyst that combines chirality and photoredox properties is not only more convenient but also more challenging and consequently, is less explored. The pioneering work

carried out by Bach's group developed the photo-asymmetric [2+2] cycloaddition by employing a chiral bifunctional catalyst, containing a chromophore unit, that induced a stereocontrol by hydrogen bond interactions.[4] A similar strategy was applied by Xiao's group who developed a bifunctional metal-photocatalyst for an enantioselective aerobic oxidation in which the photosensitizer is linked to a chiral bisoxazoline metal complex.[5] More recently, Meggers and coworkers have developed new chiral iridium and rhodium complexes that simultaneously act as photocatalysts and as chiral Lewis acids to provoke the asymmetric induction.[6] However, to the best of our knowledge, a bifunctional photo-aminocatalyst that can activate a substrate e.g. aldehyde, and a photo activatable reagent e.g. bromoalkylating reagent, has not been developed yet.

During the last few years, the asymmetric α-alkylation of aldehydes and ketones[7] has become an attractive topic because of the synthetic utility of the products obtained. In 2008, MacMillan developed a pioneering and remarkable example in which the photoredox catalyst $Ru(bpy)_3^{2+}$ and an imidazolidinone organocatalyst were employed in a cooperative manner[3a] to furnish the α -alkylation of aldehydes using different radical precursors (left, Figure 1). Since then diverse cooperative systems based on other metal complexes[8] and semiconductors[9] as photocatalysts have also been reported. Alternatively, the α-alkylation of aldehydes using metal-free photocatalysts was developed by Zeitler's[10] and Ferroud's[11] groups using the dyes Eosin Y and Rose Bengal, respectively. The combination of organic photocatalyst (Eosin Y or Rose Bengal) and MacMillan's imidazolidinone catalyst made the alkylation of aldehydes with alkyl halides possible, but the enantioselectivity achieved was lower compared to that of metal-based cooperative systems. These findings emphasize that the α-alkylation of aldehydes is not a trivial process and that there are difficulties in finding the appropriate conditions for the compatibility

of two different cooperative catalytic systems. In addition, the development of a general photo-organocatalyst for the α-alkylation of aldehydes (instead of using an external photocatalyst for each photoactivatable reagent) will be a significant advance in the field of visible light photoredox catalysis. The design of a unique metal-free catalyst – called a bifunctional photo-aminocatalyst – capable of activating both, the photoactivatable reagent and the substrate simultaneously, would be highly desirable (right, Figure 1). In the field of organocatalysis, the dual-activation of reagents by a bifunctional organocatalyst is an area of great importance, which has led to the development of novel transformations.[12] Most of the reported bifunctional catalysts are combinations of a Lewis base with a Lewis acid moiety. However, the incorporation of a photoorganocatalyst in a bifunctional catalyst is much scarcer, and more particularly, the combination of a photoorganocatalyst and an aminocatalyst has not yet been developed.[7]

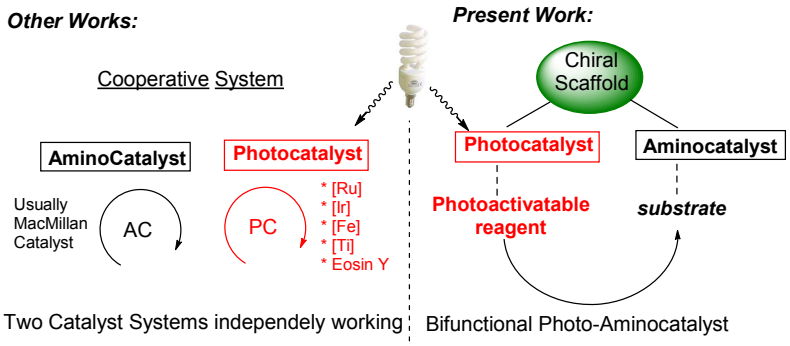

Figure 1. Comparison of the two catalytic systems, cooperative and bifunctional photo-aminocatalyst systems.

For the design of the new photo-aminocatalysts, different factors need to be taken into account (Figure 2). Firstly, the election of the chiral scaffold that will incorporate the two catalytic moieties is crucial for the success of its application. 4-Imidazolidinone has been chosen for two reasons: i) The catalysts usually employed for the alkylation of aldehydes in most of the cooperative systems are MacMillan's imidazolidinone catalysts, which are chiral 4-

imidazolidinone derivatives. ii) These catalysts possess two groups (R^1 and R^2) that could allow the incorporation of two different units (top-Figure 2). The R^1 group would permit the easy modulation of the steric hindrance of the aminocatalyst, whereas the second (R^2) would also incorporate the photocatalytic unit. Moreover, the synthesis of chiral 4-imidazolidinones is simple, short, and assembles the R^1 and R^2 groups from two separate reactants which allows an easy fine-tuning of the properties of the catalyst. Regarding the photocatalytic unit, thioxanthones have been widely studied as photoinitiators in polymerization processes,[13] and as efficient photocatalysts in energy- and electron-transfer proceses.[14] In addition, Bach's group has reported that thioxanthones can also be used as visible light-photocatalysts in asymmetric transformations.[15] We envisaged that thioxanthones would be good candidates as the photocatalytic unit for the synthesis of the bifunctional photo-aminocatalyst. In particular, 2-substituted thioxanthones were chosen as building blocks for the synthesis of the photo-aminocatalyst.[16] The second consideration is related to the geometry of the enamine in the aminocatalyst which has been studied in depth by MacMillan and others.[3] Therefore, in our case, because the incorporation of the aromatic photocatalytic unit (R^2) is required, and in order to control the geometry in the enamine, the R^1 group must be of a different relative size compared to R^2 (Bottom-Figure 1).

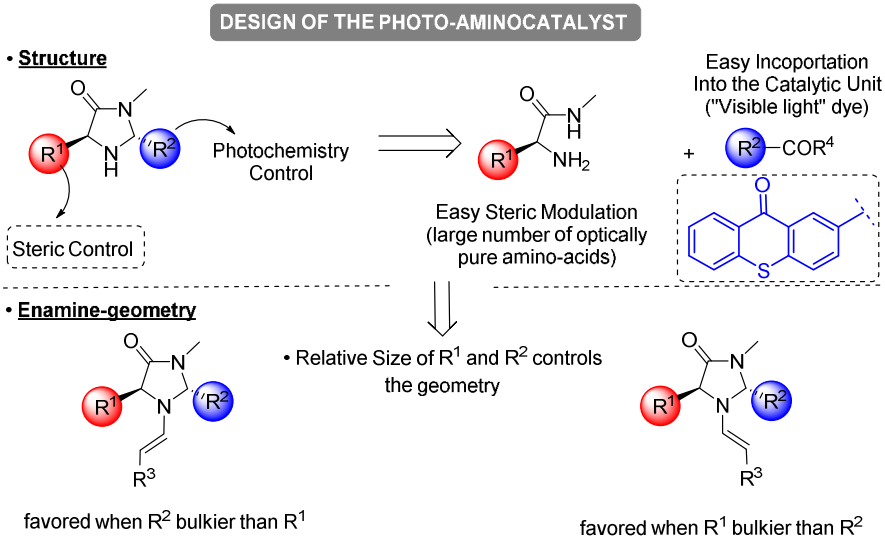

Figure 2. Design of the photo-aminocatalysts and initial considerations.

Herein, we present a bifunctional photo-aminocatalyst by a combination of both an amino-organocatalyst (imidazolidinone) and a photo-organocatalyst (thioxanthone) in the same molecule. In addition, the photophysical and electrochemical data of photo aminocatalysts, their application in the alkylation of aldehydes and a rational catalytic cycle based on different mechanistic studies, TD DFT calculations, and laser flash photolysis, are also presented.

RESULTS AND DISCUSSION

Synthesis of the Bifunctional Photocatalysts and Characterization. The photoaminocatalysts **4** were prepared in two steps, starting from commercially available aminoacids (Scheme 1). Firstly, the aminoacids **1a-c** were easily transformed into *N*-methyl aminoamides **2a-c** in high yields. The aminoacetylation of the corresponding carboxythioxanthone[17] **3** with amides **2a-c** led to the desired photo-aminocatalyst **4a-d** with moderate to good *trans/cis* ratios. The absolute configuration of the major diastereoisomer of catalysts **4b**, and **4c** was determined by single-crystal X-ray analysis[18] (see bottom Scheme 1). In

the structures both substituents (R^1 and thioxanthone) are in *trans* geometry with the thioxanthone moiety in a *pseudo*-equatorial disposition.

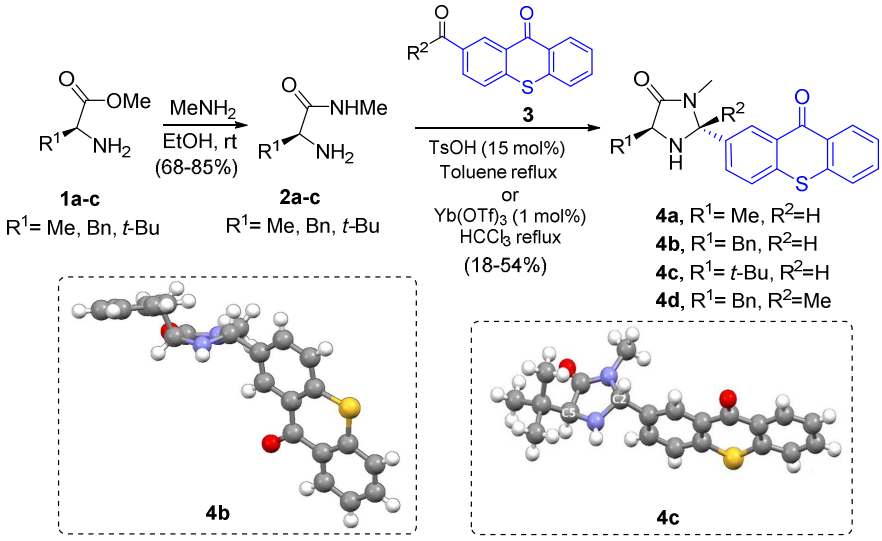

Scheme 1. Synthesis of photo-aminocatalysts **4** and X-ray crystal structure of **4b** and **4c**.

Next, we studied the photophysical and electrochemical properties of the bifunctional catalysts **4** to understand their suitability for a photocatalytic process (Table 1). For comparison the same study was also carried out using thioxanthone under identical experimental conditions. The UV-Vis absorption spectrum of thioxanthone presents a maximum absorption maximum at λ_{max} = 381 nm with a significant part of the absorption band in the visible region. The different structures and stereochemistry of the amino-thioxanthone catalysts **4** showed little effect on the maximum absorption (λ_{max} = 380 ± 1 nm). Similar findings were described by Neumann *et al.* who reported that the 2-substitution in the aromatic ring of the thioxanthone did not produce any significant effect on the absorption maximum, or on the molar absorption coefficients, regardless of the nature of the substituent.[16] Moreover, strong emissions at λ_{max} = 413-420 nm were observed for all catalysts upon photoexcitation of the absorption maximum at room temperature. The excited singlet state energy of the photoaminocatalyst was estimated at the intersection of

the normalized absorption and emission spectra. As we expected, all the S1 energy values are very close to that of thioxanthone, which indicates that the imidazolidinone fragment has little effect on the photophysical properties of the thioxanthone moiety.

The ground-state redox potentials of the catalysts were determined by cyclic voltammetry (CV) in acetonitrile as solvent (Table 1). Amino-thioxanthone catalysts **4** show two irreversible oxidation peaks: the most positive corresponds to the oxidation of the thioxanthone moiety and the less cathodic to the amine moiety (see S.I. for further details). This assignment was confirmed by comparing the redox values of the bifunctional catalysts **4** with the oxidation peaks of thioxanthone and imidazolidinone catalysts **4f** (1.40 V vs. SCE in CH_3CN). In addition, one reversible reduction potential was also determined, which corresponds to the thioxanthone reduction. Taking into account the redox potentials and the singlet state energy, the oxidation and reduction excited state potentials of catalysts **4** were estimated. Both, oxidation and reduction potentials in the excited state of the bifunctional catalysts **4** are similar to those calculated for thioxanthone which indicates the preservation of the electrochemical properties of the thioxanthone moiety on the bifunctional catalyst properties, which confirms the adequate design of the bifunctional catalysts **4**.

Table 1. Photophysical and electrochemical data of thioxanthone and catalysts **4a-d**, and structures of parent imidazolidinone catalyst **4e** and **4f**.

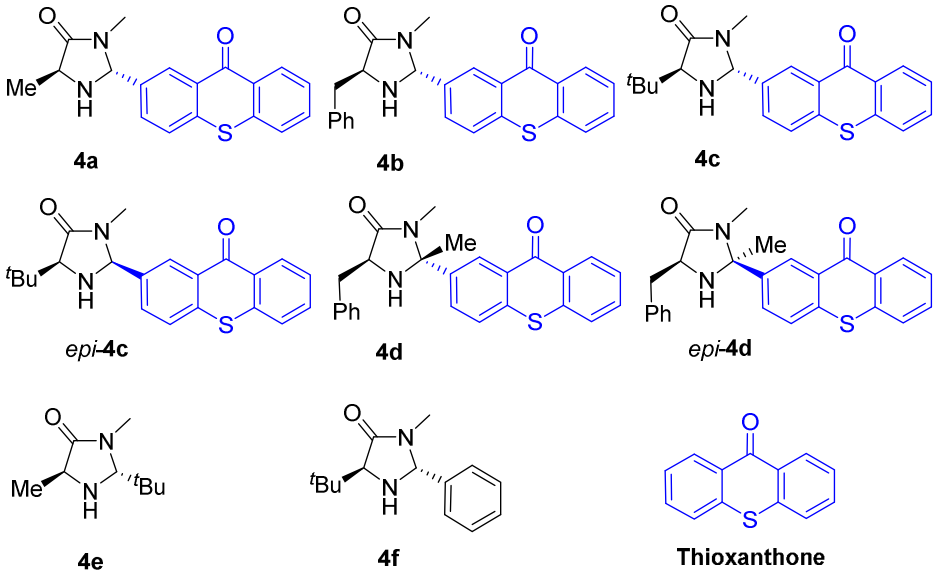

Compound	Absorption (λ_{max}, nm)[a]	Emission (λ_{max}, nm)[b]	S_1 Energy (eV)[c]	E_{ox} (V vs SCE)[d]	E^*_{ox} (V vs SCE)[e]	E_{red} (V vs SCE)[d]	E^*_{red} (V vs SCE)[e]
Thioxanthone	381	409	3.13	+1.82	-1.31	-1.48	+1.65
4a	381	412	3.14	+1.32 +1.83	-1.31	-1.45	+1.69
4b	381	416	3.12	+1.44 +1.80	-1.32	-1.50	+1.62
4c	381	413	3.13	+1.36 +1.80	-1.33	-1.50	+1.63
epi-**4c**	379	420	3.14	+1.08 +1.82	-1.32	-1.35	+1.79
4d	380	414	3.13	+1.49 +1.84	-1.29	-1.44	+1.69
epi-**4d**	379	413	3.15	+1.50 +1.84	-1.31	-1.41	+1.74

[a] UV-Vis spectra recorded in 0.025 mM CH_2Cl_2 solutions at rt. [b] Fluorescence recorded in 0.25 mM CH_2Cl_2 solutions at rt. [c] Determined from the intersection of the normalized absorbance and emission spectra (converted into eV). [d] Conditions: 50 $mV \cdot s^{-1}$ scan rate; 1 mM solution of compound in argon-saturated CH_3CN solution; 0.1 M solution of Bu_4NPF_6; glassy carbon disk (2.8 mm diameter) as working electrode; platinum wire as counter electrode; Ag/AgCl as reference electrode. [d] Excited state redox potentials of the thioxanthone moiety estimated using the equation: $E^*_{ox} = E_{ox} - E_{0\text{-}0}$ or $E^*_{red} = E_{red} + E_{0\text{-}0}$, where $E_{0\text{-}0}$ is the singlet state energy.

In order to corroborate the experimental photophysical observations, the ground state geometry optimization of thioxanthone and the bifunctional catalyst **4c**, as well as their energy transition studies, were optimized by TD DFT calculations (see Figure 3 and S.I.). Geometry optimization of the thioxanthone ground state (S_0) revealed a planar structure with C_{2v} symmetry similar to that previously described in the literature (right, Figure 3).[19,20] Other possible conformations such as non-planar structures with C_s symmetry described by Rubio Pons *et al.*[21] were not considered because they are less stable conformations.[22] The absorption spectra of thioxanthone exhibited a first band located at 381 nm that, by taking our calculations into account, can be assigned to the π-π^* transitions from HOMO to LUMO orbitals (see S.I. for further details). In addition, an n-π^* optically forbidden transition (S2), energetically close-lying to S1 was also observed, which is in agreement with Ishijima's studies.[23] On the other hand, Mundt *et al.*[19] observed a change in the energy of these excited states with a lower n-π^* transition in vacuum conditions. These variations are due to the solvent effect, which stabilizes the π-π^* excited state of the thioxanthone. In addition, the optimization of the triplet state leads to an energy of 2.73 eV that is close to the experimental value of 2.84 eV.[24] As described above (see Table 1), the UV-vis of **4c** depicts a similar profile to thioxanthone (see left, Figure 3). The TD-DFT calculations showed that S1 transition takes place between the HOMO, which is delocalized over the whole molecule with a contribution from the amine moiety, and the LUMO localized predominantly on the

thioxanthone (Figure 3). We found that the triplet state of **4c** exhibited an energy value of 2.73 eV, which is identical to that of free thioxanthone.

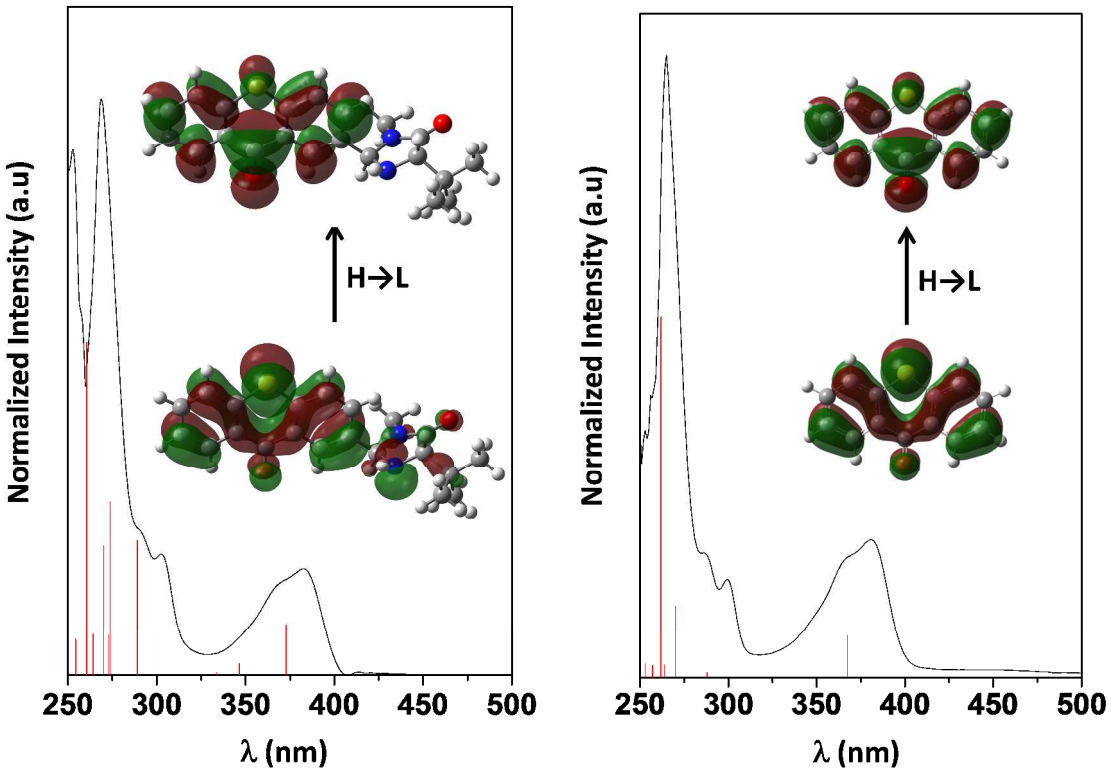

Figure 3. Comparison between the experimental (black line) and the calculated vertical (red bars) excitation by TD-DFT B3LYP (6-311++G**) for catalyst **4c** (left), using DMF as solvent, and thioxanthone (right) using DCM as solvent. Inset: Molecular orbitals involved in the S1 transition.

The α-alkylation of aldehydes with diethyl bromomalonate was chosen as a model reaction[3a] to evaluate the catalytic activity of the bifunctional photocatalysts **4** (see below, Table 2). Moreover, using the usual formulation for the determination of the free energies of a photoinduced electron transfer (PET) process ($\Delta G_{PET} = 23.06[E_{ox} - E_{red}] - E^*(S_1 \text{ or } T_1)$), we can estimate the thermodynamic driving force of the PET between the diethyl bromomalonate as the

reactant *vide infra* (E_{red} = - 1.0 V vs. SCE in CH_3CN) and catalysts **4** (see E_{ox} and E^* values in Table 1). All the estimated ΔG_{PET} values are negative (ranging from -9.0 to -9.9 Kcal/mol) which indicates that the process is thermodynamically favorable for all the catalysts **4**.

Optimization Studies and Scope of the Reaction

Initially, the α-alkylation of hydrocinnamaldehyde (**5a**) was carried out using MacMillan's imidazolidinone catalyst **4e** (20 mol%) in combination with $Ru(bpy)_3^{2+}$ (1 mol%) as a photocatalyst (entry 1) under visible light irradiation (23 W commercial fluorescent bulb) using DMF as solvent. The reaction furnished the α-alkylated product **7a**, working with Ru catalyst and **2e** in a comparative manner, with an 85% conversion and a 91% enantiomeric excess as reported in the literature.[3a] The catalyst **4f** was then employed in the same reaction conditions obtaining a lower conversion (59%) and a higher enantioselectivity (97%). We then tested our bifunctional photocatalyst **4a-d** (entries 3-13). To our delight, the bifunctional photocatalyst **4a** allowed the synthesis of **7a** with complete conversion and a moderate enantiomeric excess (64% ee, entry 3). The use of catalyst **4b** with a slightly bulky substituent, such as the benzyl group (R^1= Bn), provided comparable enantioselectivity (57%, entry 4), whereas the catalyst with the bulkier *tert*-butyl moiety (**4c**) achieved an outstanding >99% ee and full conversion (entry 5). By contrast, the epimer photocatalyst *epi*-**4c** showed very low reactivity and enantioselectivity (entry 6). Furthermore, catalysts **4d** and *epi*-**4d** with a quaternary stereocenter showed lower enantiomeric excesses and conversions than catalyst **4c** (entries 7-8). Using the best catalyst **4c**, other solvents such as DMSO or CH_2Cl_2 were also studied, obtaining in all cases identical enantioselectivities, but lower conversions (entries 9-10). Conversely, an apolar solvent such as toluene afforded the product with a low conversion (entries 11-12). Finally, the reduction of the catalyst loading involved a strong conversion decrease (entry 13) and the use of blue LEDs

(λ_{max}= 450 nm) as an irradiation source afforded aldehyde **7a** in lower enantioselectivity (entry 15).

Table 2. Screening of different bifunctional photo-organocatalysts **4** in the α-alkylation of aldehyde **5a**.[a]

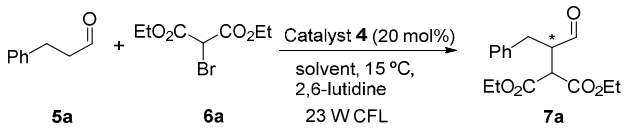

5a **6a** **7a**

Ent.	Catalyst (x mol%)	Solvent	Conv.[b] (%)	ee (%)[c]
1	**4e** (20) + $Ru(bpy)_3^{2+}$ (1)	DMF	85	91
2	**4f** (20) + $Ru(bpy)_3^{2+}$ (1)	DMF	59	97
3	**4a** (20)	DMF	100	64
4	**4b** (20)	DMF	77	57
5	**4c** (20)	DMF	100	>99
6	epi-**4c** (20)	DMF	11	8[d]
7	**4d** (20)	DMF	71	37
8	epi-**4d** (20)	DMF	30	29
9	**4c** (20)	DMSO	60	>99
10	**4c** (20)	CH_2Cl_2	14	>99
11	**4c** (20)	Toluene	5	96
12	**4c** (10)	DMF	35	91
13[e]	**4c** (20)	DMF	100	70

[a] **5a** (0.3 mmol), **6a** (0.15 mmol), 2,6-lutidine (0.3 mmol) and catalyst **4** in 0.3 mL of the indicated solvent were stirred at 15 °C for 18 h under visible light irradiation (CFL-23 W). [b] Conversion of **7a** determined by ^{1}H NMR. [c] Determined by SFC on chiral stationary phase after derivatization (see S.I.). [d] Opposite enantiomer obtained. [e] Reaction carried out under blue LED (15 W) irradiation. Conv. Conversion.

Once the optimal conditions had been determined (entry 6, Table 2), we studied the scope of the α-alkylation of aldehyde **5a** using a variety of alkylating reagents (Table 3). Bromomalonates **6a** and **6b** (a tertiary bromide) were reduced by catalyst **4c** to give aldehydes **7a** and **7b** with an excellent yield and enantioselectivies. Later, the electron reduction of bromo-nitrile species (bromoacetonitrile, E_{red}= -1.23 V vs SCE in CH_3CN, see S.I. for the cyclic voltammetry) by the photo-organocatalyst **4c** was explored, and the negative value of the free energy (ΔG_{PET}= -2.3 Kcal/mol) guarantees the thermodynamic driving force of the process. The reaction with nitriles **6c** and **6d** provided the aldehydes **7c** and **7d** respectively, in high yields and excellent enantioselectivities. It is worth mentioning that these results are better than those previously described in the literature.[7] α-Bromoketone derivatives **6e-g** (e.g. bromoacetophenone, E_{red}= -0.89 V vs SCE) were also reduced using our catalytic system, yielding the ketones **7e**, **7f** and **7g**, respectively, with an excellent yield and high levels of enantiocontrol (84-95% ee). By contrast, the bromobenzyl derivatives were more difficult to reduce (E_{red}= -1.40 V vs SCE, see cyclic voltammetry in S.I.). The estimated ΔG_{PET} value for the bromomethylbenzene reagent is +1.59 V, which indicates that the process is thermodynamically endergonic. As expected, the reaction with bromomethylbenzene did not take place under the optimized conditions. The introduction of electron-withdrawing groups at the aromatic ring decreased the potential reduction of the benzyl substrates and consequently, the reaction of the benzyl derivative **6h** with aldehyde **5a** was successfully catalyzed by the bifunctional thioxanthone **4c** to afford **7h** in 97% ee.

Table 3. Scope of the α-alkylation of **5a** with bromoderivatives **6**.

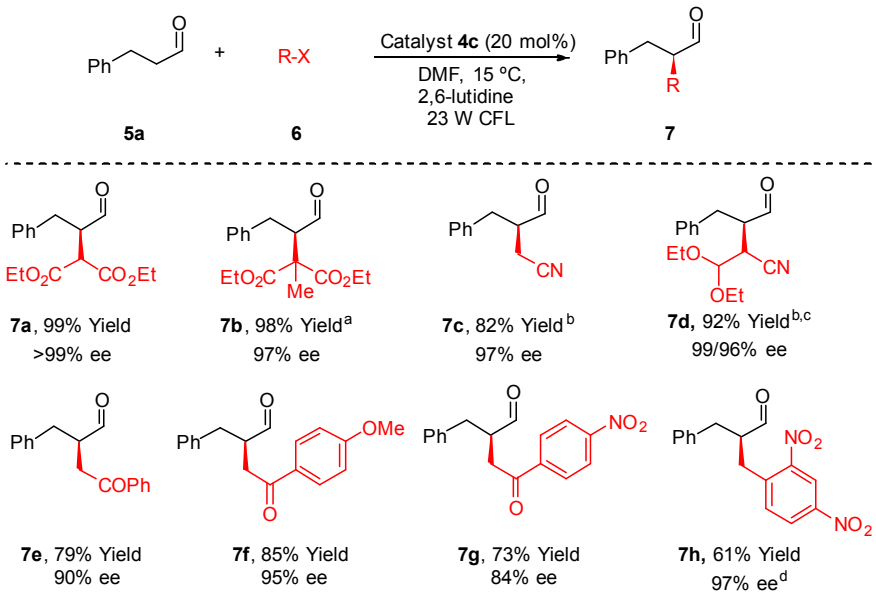

[a] Based on a 30% conversion by ^{1}H NMR. [b] 5 eq. of **5a** and DMSO used as solvent. [c] Overall yield of both diastereoisomers (dr 2:1). [d] DMSO used as solvent.

Next, the applicability of the photocatalyst was evaluated using different aldehydes (**5**) with bromomalonate **6a** as bromo-derivative (Table 4). Primary and secondary β-alkyl-aldehydes **5i** and **5j** exhibited good reactivity, affording the corresponding aldehydes **7i** and **7j** with excellent enantioselectivies (96% and 97% ee, respectively). To the best of our knowledge, these enantioselectivies are the highest reported in the literature for those substrates.[7] The bifunctional catalytic system also allowed the successful alkylation of functionalized aldehydes **1k** and **1l**. Accordingly, the alkylated-aldehydes **7l** and **7k**, containing an *N*-Boc-piperidine and a double bond respectively, were isolated in good yields and high enantioselectivities (96% and 99% ee, respectively). It must be highlighted that the level of enantioselectivity achieved for the α-

alkylation of aldehydes using the bifunctional catalyst **4c** are not only comparable, but also better than those reported in the literature using other cooperative systems.

Table 4. Scope of the reaction of different aldehydes (**5**) with diethyl bromomalonate (**6a**).

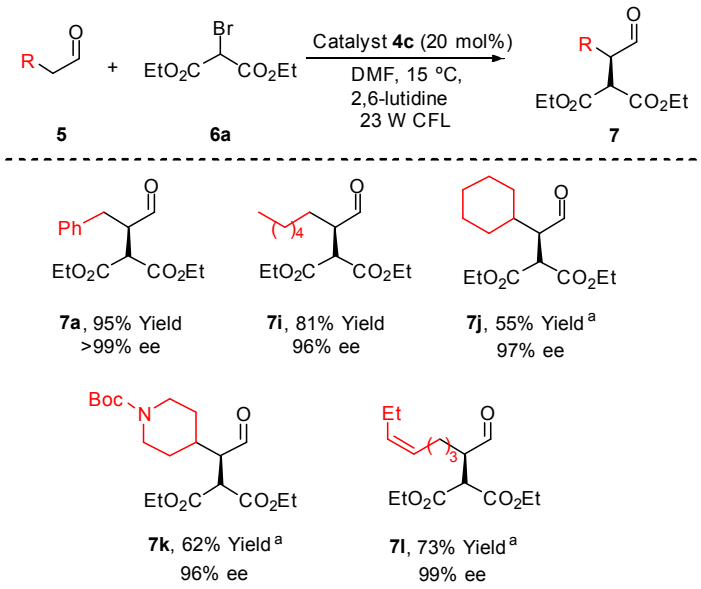

[a] 5 eq. of the corresponding aldehyde **5**.

Mechanistic Considerations

General Accepted Photo-Catalytic Cycle: According to the original mechanism proposed by MacMillan and others,[3,7-11] we postulate the mechanism outlined in Scheme 2 for the photoalkylation of aldehydes using the bifunctional catalyst **4c**. The reaction starts with the condensation of catalyst **4c** with aldehyde **5** to give the first enamine intermediate **A**. The thioxanthone moiety of intermediate **A** can absorb light to reach the excited intermediate **A*** (step 1). It is well-known that thioxanthones can promote a single electron transfer process (SET).[14] Therefore, this excited intermediate **A*** can reduce the bromo-alkane derivative **6** (step

2) through a SET reduction, to give intermediate **B** and the alkyl radical. Then, the alkyl radical is added to the nucleophilic enamine **B** to obtain the α-amino radical **C** that can be intramolecularly oxidized by the thioxanthone radical-cation. Finally, the resultant iminium **D** is hydrolyzed to give the final α-alkylated aldehyde **7**. In order to confirm this mechanistic proposal, different experiments involved in the process, and related to the different steps, were carried out.

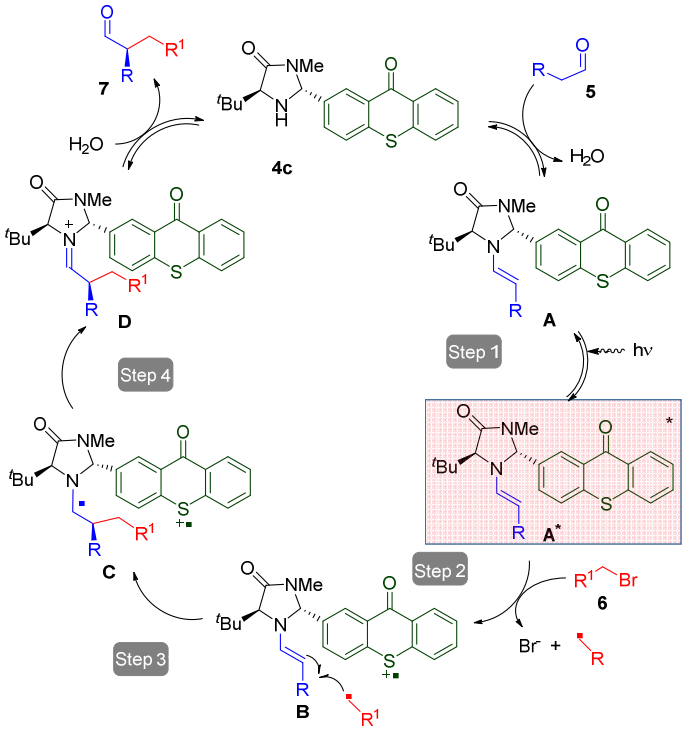

Scheme 2. Original proposed mechanism by MacMillan for the photocatalytic α-alkylation of aldehydes.[3a]

Initiation Process (Step 2): Three different mechanisms have been proposed in the literature for the photochemical initiation process of this reaction, depending on the organocatalyst employed, the presence of an external photosensitizer, and/or the type of bromo-derivative (Scheme 3). The first was proposed by MacMillan[3] and coworkers for the cooperative catalytic

system, using iridium(III) or ruthenium(II) complexes and MacMillan's imidazolidinone catalyst (top-left, Scheme 3). In this case, the reducing excited state of the metal photocatalyst is able to reduce the bromoalkane thought a SET process, giving the radical intermediate **I** (top-left, Scheme 3). The second mechanism was described by Melchiorre *et al.*[25] In the latter case, a colored EDA complex intermediate between the enamine and a benzylbromide is formed and can be photoexcited to give a SET from the enamine to the bromobenzyl derivative obtaining the radical intermediate **II** (bottom-left, Scheme 3). The third and most recent mechanism proposed is related to the direct photoexcitation of the enamine,[26] generated upon condensation of an aldehyde and Jørgensen-Hayashi's catalyst, which is able to reach an excited state and to undergo a SET with bromo malonates to form the radical intermediate **I** (Right-Scheme 3). Once the radical intermediate **I** or **II** was formed by some of these mechanisms,[27] the enamine can trap the intermediate (**I** or **II**) as described in step 3 of Scheme 2.

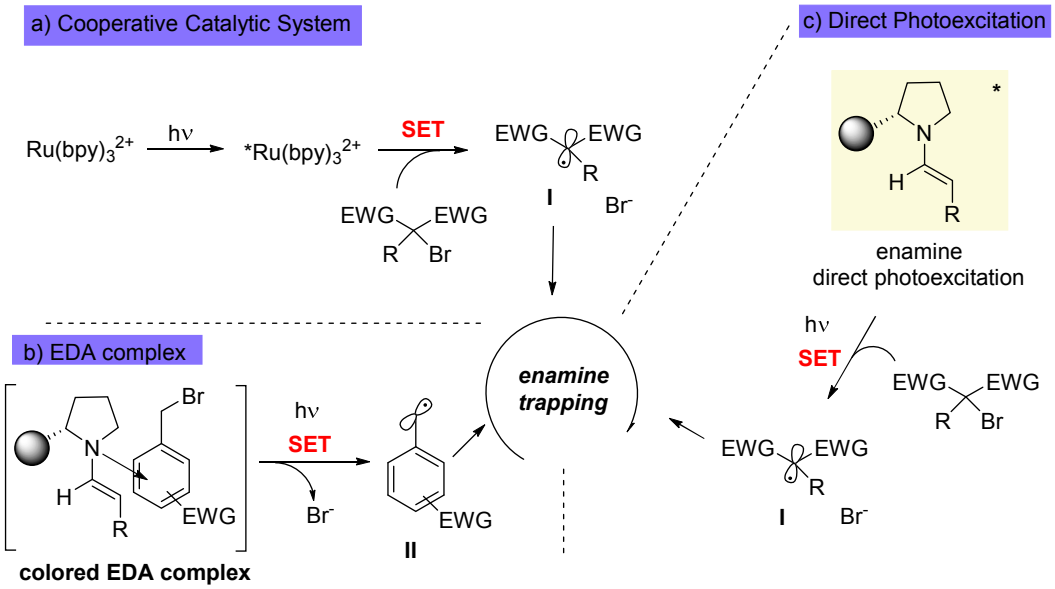

Scheme 3. Three different pathways for the initiation process of the α-alkylation of aldehydes.

In order to distinguish which of the initiation mechanisms from the three different pathways was applicable, and to elucidate the role of the thioxanthone in our catalytic system, we studied the α-alkylation of hydrocinnamaldehyde using three different catalysts **4e**, **4f** and **4g** (Scheme 4). We chose diethyl bromomalonate as the reagent in order to discard the EDA complex type mechanism because this requires an electron deficient bromobenzyl (equation b, Scheme 3). Catalyst **4f** was chosen because it has an aromatic substituent with a similar steric hindrance around the secondary amine active center compared to that of our bifunctional catalyst (**4c**), but without the thioxanthone moiety. The results obtained using **4f** will allow us to distinguish the role of the thioxanthone moiety in the bifunctional catalyst **4c**. In addition, the imidazolidinone catalyst **4e** and Jørgensen-Hayashi's catalyst (**4g**) were also studied for comparison with the mechanisms reported in the literature.[3,27] Firstly, the reaction was carried out in the presence of catalyst **4e-g**, without any external photocatalyst (Scheme 4). As Melchiorre reported,[25] the Jørgensen-Hayashi catalyst **4g** and catalyst **4e** afforded the alkylated product **7a**, with 100% and 41% conversion respectively, due to the photoexcitation of the intermediate enamine (equation c, Scheme 3). By contrast, catalyst **4f** did not produce any alkylated product while a 41% conversion was obtained with the MacMillan's catalyst **4e**. This last result seems to indicate the possible photo-absorption of the enamine generated upon the condensation of aldehyde **5e** and catalyst **4e.** On the other hand, the addition of the ruthenium(II) complex as an external photocatalyst in combination with aminocatalyst **4e** or **4f** increased the formation of the α-alkylated product **7a** up to 85% and 59%, respectively. These results would indicate that the enamine formed upon condensation of catalyst **4f** and aldehyde **5a** is not able to generate the alkyl radical (through a SET between the photoexcited enamine and the bromo derivative) and that the reaction needs an external photocatalyst to proceed.

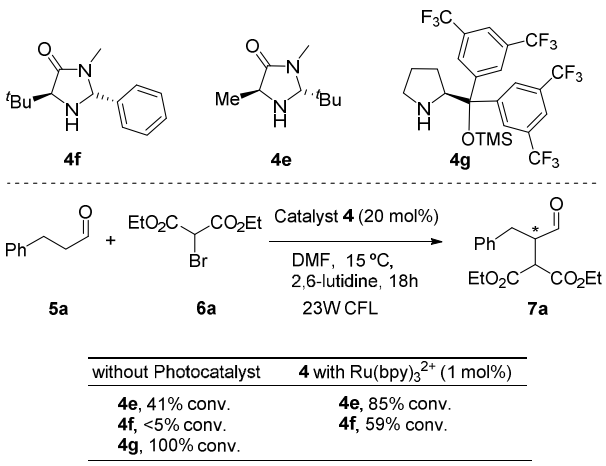

Scheme 4. α-Alkylation of hydrocinnamaldehyde using catalyst **4e**, **4f** and **4g** in the absence and presence of external photocatalyst.

To obtain more information and to understand the differences in terms of the reactivity in the reaction conducted with catalyst **4e**, **4f** and **4g**, three different enamines (**4e-En**, **4f-En** and **4g-En**, Figure 4)[28] were synthesized by condensation of phenylacetaldehyde with the different aminocatalysts.[27] CV and UV-Vis spectra of the enamines were performed and the excited redox potentials of the enamines were calculated (see S.I. and Figure 4). According to the excited reduction potential of the three enamines (E^*_{red} from - 2.38 to -2.74 V vs SCE in CH_3CN), all should be able to reduce the diethyl bromomalonate (E_{red} = - 1.0 V vs. SCE in CH_3CN) without the need of an external photocatalyst. The UV-Vis spectra of the enamines were also compared. Enamine **4g-En** derived from the Jørgensen-Hayashi´s catalyst has a significant absorption around 400 that guarantees the visible light absorption of the enamine, which can act as photoinitiator and reduce the bromomalonate **6a** via direct photooxidation without the addition of an external photocatalyst. However, this cannot be the reason for the different behavior between the enamines **4e-En** and **4f-En** since they have almost identical UV-Vis absorption spectra but a different reactivity (41% vs <5% conversion, respectively). However, an additional factor must

to be involved in the null conversion obtained in the case of catalyst **4f** (with a phenyl substituent). We think that in the case of catalyst **4f** the steric hindrance of the phenyl group is responsible for the lack of any initiation process needed to generate the alkyl radical from the bromo derivative through the direct photoexcitation of the enamine. The addition of an external photocatalyst in combination with **4f** overcomes the null contribution of the direct photoexcitation of the enamine, enabling the initiation step of the reaction to give good conversions in both cases (59% and 85%, Scheme 4). Therefore, taking into account that catalyst **4f** and the bifunctional catalyst **4c** possess a similar steric hindrance around the secondary amine active center, we assumed that the thioxanthone group is responsible for any initiation step process in the case of the bifunctional catalyst **4c**.

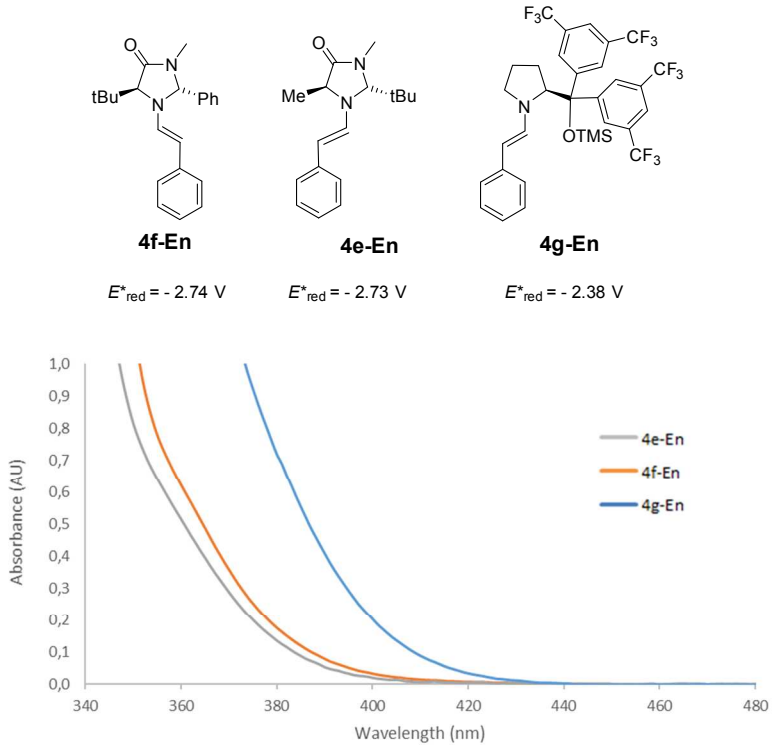

Figure 4. Spectroscopic and CV studies of enamines **4e-En**, **4f-En** and **4g-En** (V vs SCE in CH_3CN).

Catalyst steric effects in the initiation process: As described previously, the reaction under catalyst **4f** led to a null conversion of the final aldehyde **7a**, whereas the alkylation took place with 100% conversion under catalyst **4c** (Scheme 5). Since we thought that the steric hindrance around the active center of the catalyst is mainly responsible for the different reactivities observed, some additional experiments were performed. It is well known that the SET process proceeds between two spatially close molecules (enamine and bromomalonate derivative), and therefore, the steric factor around the enamine must play an important role in the initiation process. With these ideas in mind we synthetized a variety of imidazolidinone catalysts **4e-i** and performed the alkylation under the same reaction conditions (see Scheme 6).

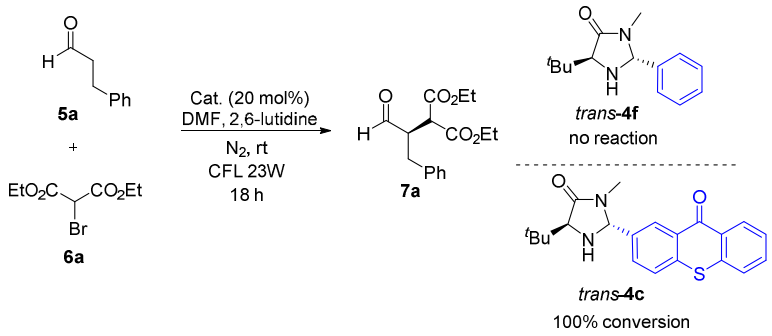

Scheme 5. α-Alkylation of hydrocinnamaldehyde using catalyst **4f** and **4c**.

Firstly, we carried out the reaction using each catalyst **4**, without the addition of an external photocatalyst, with the aim of identifying the effect of the steric hindrance of the intermediate enamine on the initiation process. Regarding the catalysts in *trans*-configuration, the conversions obtained using the different catalysts *trans*-**4** show that only the catalyst with the smallest substituent (methyl, *trans*-**4e**) is able to promote the initiation of the reaction by direct photoexcitation of the enamine. The *trans*-disposition of the substituents shielded both faces of the enamine (Scheme 6), and as a consequence the bulkiest catalysts (*trans*-**4f**, *trans*-**4h** and *trans*-**4i**) inhibit the SET process from the enamine to the bromoderivative **6a**. In these cases, the

addition of $Ru(bpy)_3^{2+}$ as an external photocatalyst responsible for the photo-initiation step, overcame this inhibition and allowed the reaction to progress with all the catalysts except in the case of the bulkiest catalyst *trans*-**4i** and *cis*-**4i**, indicating that the corresponding enamines *trans*-**4i-En** and *cis*-**4i-En** were not formed.

Conversely, it is well known that enamines formed from imidazolidinones with substituents in *cis*-orientation have one of the faces unblocked (bottom, Scheme 6). Therefore, phenyl and cyclopropyl catalysts *cis*-**4f** and *cis*-**4h** were able to carry out the α-alkylation of aldehydes even in the absence of an external photocatalyst because the enamine and the bromo derivative can come into closer proximity compared to the case of the *trans*-catalysts. Although the reactivity of catalysts *cis*-**4** was higher than the corresponding *trans*-**4**, their enantiomeric discrimination was poor and for this reason these *cis*-catalysts are not usually employed in photo-aminocatalysis.[3,7] To conclude this section, the initiation step under the bifunctional catalyst **4c** proceeds towards the thioxanthone moiety and the electronic transfer between the enamine and the bromo derivative can be discarded.

	trans-4e	trans-4f	trans-4h	trans-4i
Conv. (without photocat)	41%	<5%	0%	0%
Conv. (with [Ru])[a]	85%	59%	82%	0%
		cis-4f	*cis*-4h	*cis*-4i
Conv. (without photocat)		25%	18%	0%
Conv. (with [Ru])[a]		47%	80%	3%

[a] 1 mol% of $Ru(bpy)_3^{2+}$ was added

Scheme 6. Effect of the size and disposition of the catalyst substituents in the α-alkylation of aldehydes.

Propagation Process and Quantum Yields: In the α-alkylation of aldehydes, Yoon[29] and Melchiorre[27] have shown that a chain propagation mechanism is involved in the reaction. According to these studies, the mechanism of the alkylation of aldehyde is outlined in Scheme 7. The radical **I** is trapped by enamine **II** to form the α-amino-radical **III** that can be oxidized by the bromo derivative **6**. Next, the iminium ion **IV** generated is hydrolyzed to recover catalyst **4**. Therefore, the generation of additional radical species to react with **II**, via the initiation process, is unnecessary since propagation of the process can take place (**6** to **I**). Yoon and Melchiorre

have demonstrated the propagation processes by quantum yield measurements (Φ). In Melchiorre's photocatalytic system, the Jørgensen-Hayashi's catalyst presented a Φ = 18,[26] whereas Yoon reported that the MacMillan´s catalyst had a Φ = 22 in this photocatalytic system.[27]

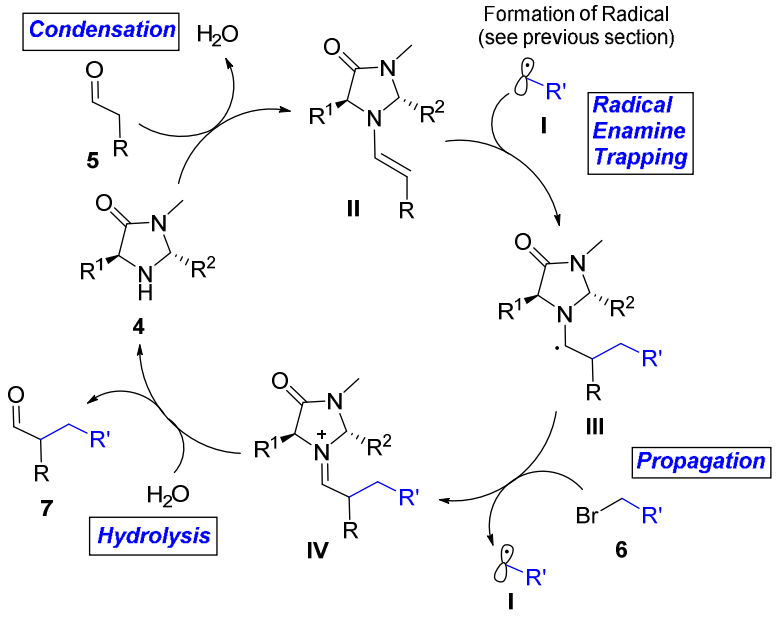

Scheme 7. Proposed radical-chain propagation process for the α-alkylation of aldehydes.

In order to study the propagation process of our photocatalytic system, we measured the quantum yield of the overall reaction with the bifunctional catalyst **4c**. Using our irradiation system, the quantum yield of catalysts **4g**, and **4e** or **4f** with thioxanthone as the external photocatalyst was also determined (Figure 5). The quantum yields were measured by the ferrioxalate actinometer methodology, following the procedure described by the IUPAC.[30] A quantum yield of 9.2 was obtained in the reaction catalysed by Jørgensen-Hayashi's catalyst (**4g**) under our irradiation system (Figure 5). This datum is lower than that reported by Melchiorre due to the different reaction and irradiation conditions, but is in agreement with a self-propagation mechanism (Φ > 1). For catalysts **4e** and **4f**, quantum yields of 5.6 and 4.4 respectively, were

measured using thioxanthone as external photocatalyst. By contrast, a quantum yield of 2.4 was obtained using our bifunctional catalyst **4c**. This reduction in the overall quantum yield, in the case of our bifunctional catalyst **4c**, can also be attributed to the contribution of the internal redox process (the oxidation of the α-amino-radical and the reduction of the radical cation thioxanthone; see intermediate **C**, step 4 in Scheme 2). Therefore, an additional SET between the thioxanthone group of catalyst **4c** and the bromoderivative to initiate the catalytic cycle is necessary (step 2, in Scheme 2) which leads to a further decrease in the quantum yield value observed.[31]

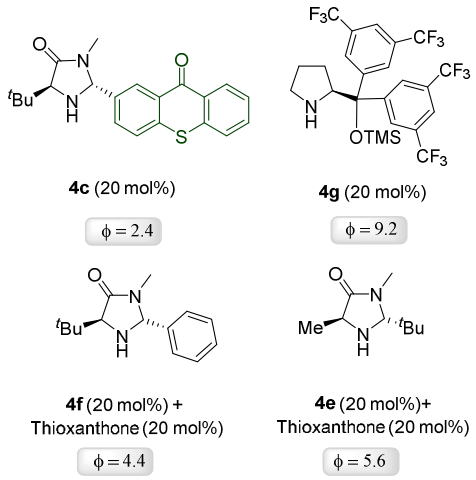

Figure 5. Overall quantum yield of the α-alkylation of hydrocinnamaldehyde with diethylbromomalonate using different catalytic systems.

Laser flash photolysis experiments: In order to gain further insight into the mechanism, laser flash photolysis experiments (LFP) were performed to investigate the excited state of bifunctional catalyst **4c** involved in the process, and its comparison with thioxanthone. The transient spectrum of thioxanthone in deoxygenated DMF shows an absorption maximum at 630 nm, which corresponds to the characteristic triplet-triplet band of thioxanthone.[32] Next, we focused our attention on the kinetic decays of both compounds at 630 nm (Figure 6). The decays

of catalyst **4c** and thioxanthone were markedly different, with triplet lifetime values (τ) much higher for thioxanthone (1.879 μs) than for the bifunctional photocatalyst **4c** (0.682 μs). Therefore, the triplet quenching rate constant (k_q) was determined to be 9.3 x 10^5 s^{-1}. These results can be explained based on the photochemical studies of thioxanthones as photoinitiators in the polimerization of olefins.[13] In these studies, the thioxanthone triplet excited state is quenched by amines given the corresponding di-radicals by an electro-transfer mechanism (Scheme 8). This intermediate could undergo decomposition via proton transfer from the amino-radical to the ketone radical or back-electron transfer (BET) to the ground state. We have experimentally confirmed that the degradation of **4c** was negligible, confirming the rapid BET process. Similarly, a decrease in the fluorescence emission of the bifunctional catalyst compared to that of thioxanthone was also observed due to deactivation by the amino moiety (see S.I.).

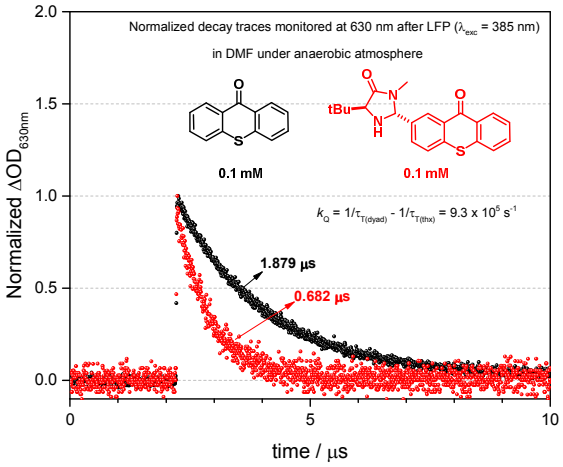

Figure 6. Normalized triplet decay traces of thioxanthone and catalyst **4c** at 630 nm (λ_{exc} = 385 nm).

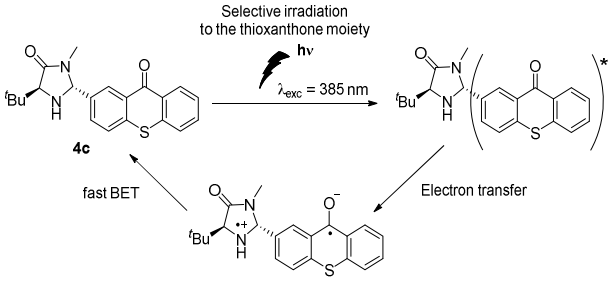

Scheme 8. Deactivation mechanism of the bifunctional catalyst **4c**.

We then studied the effect of the enamine formation on the decay of catalyst **4c**. As an indirect proof, we subjected a solution of catalyst **4e** to LFP in the presence and absence of hydrocinnamaldehyde (Figure 7).[28] After the addition of the aldehyde the solution was allowed to stabilize for 20 minutes. We observed an enhancement of the optical density monitored at 630 nm together with longer temporal profile after the enamine formation. These results seem to indicate that the formation of the enamine could retard the intramolecular electron-transfer process, increasing the amount of thioxanthone triplets. Moreover, the fluorescence of the catalyst **4c** after the addition of increasing amounts of aldehyde showed a bathochromic shift and an enhancement of the maximum emission (see S.I. for graphs). All these experiments demonstrate that the intramolecular quenching of the excited state (singlet or triplet) of the thioxanthone moiety by the amino group in the bifunctional catalyst, is reduced after the enamine formation.

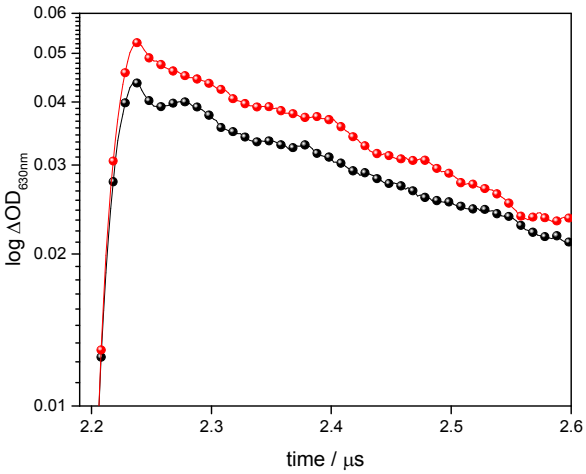

Figure 7. Temporal profiles of catalyst **4c** in deoxygenated DMF monitored at 630 nm (λ_{exc} = 385 nm) in the absence (black) and in the presence (red) of hydrocinnamaldehyde after 20 min. stabilizing.

All these experimental studies are in agreement with our TD-DFT calculations. The calculations for the **En-4c** intermediate show a behaviour similar to that of the bifunctional catalyst **4c**, but in this case the main electronic transitions are from the HOMO-1 orbitals mainly localized over the enamine moiety to LUMO in the thioxanthone (Figure 3). These studies also confirm the presence of a HOMO-LUMO transition in the visible range (484 nm) but with a low oscillation strength. The triplet state shows an energy value of 2.74 eV, which is the same as **4c.** In addition, a synergetic effect on the catalyst that leads to a photo-induced charge transfer from the enamine to the thioxanthone is observed, where the carbonyl group could play an important role.

Once it had been established that the enamine derivative (**4c-En**) was a relevant intermediate for the reaction mechanism, we carried out quenching investigations to disclose the nature of the thioxanthone excited state involved in the photoinduced electron transfer mechanism.

Fluorescence studies of the bifunctional catalyst **4c** in the presence of diethyl bromomalonate do not afford any change in the intensity or shape of the emission spectra (see S.I.). In addition, the triplet decay at 630 nm, in the presence of increasing amounts of diethyl bromomalonate, revealed a dynamic quenching. The corresponding rate constant $k_q(T_1)$ was determined from the decay traces obtained for the T-T absorption of **4c** in the presence of increasing amounts of **6a** (Figure 8A). By plotting the reciprocal lifetime ($1/\tau$) against the concentration of **6a**, a linear relationship was obtained (Figure 8B). The slope of the straight line was 6.4 x 10^6 M^{-1} s^{-1}, which corresponds to $k_q(T_1)$ according to the following equation: $1/\tau = k_0 + k_q(T_1)$[**6a**]. Furthermore, the end-of-pulse absorption in all measurements was clearly the same, being in complete agreement with the emission experiments previously described. In conclusion, the combination of fluorescence and LFP studies indicate that the electron transfer process takes place from the triplet excited state of the thioxanthone moiety of the bifunctional catalyst **4c**.

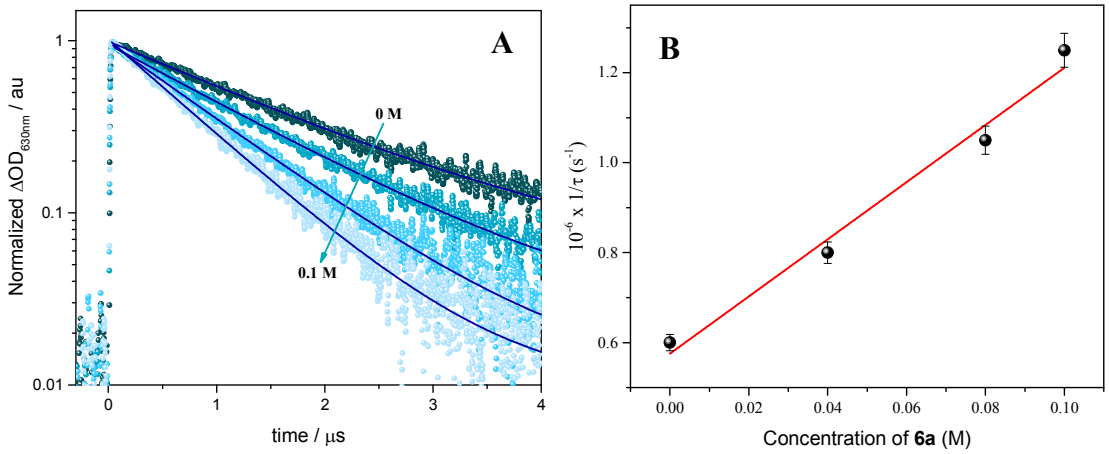

Figure 8. A: Normalized decay traces of the T-T absorption of **4c** (0.1 mM in N_2/DMF, λ_{exc} = 385 nm) monitored at 630 nm in the presence of increasing amounts of diethyl bromomalonate (**6a**). The blue lines indicate the goodness of the lifetime measurement. **B:** Plot of $1/\tau$ against concentration of **6a** to obtain $k_q(T_1)$; experimental errors were lower than 3% of the values obtained.

CONCLUSIONS

In this work we have developed a new bifunctional photoaminocatalyst based on imidazolidinone and thioxanthone in a two-step synthesis, which allows an easy tuning of the steric properties. The photophysical and electrochemical data of the imidazolidinone photocatalyst have been determined, indicating that the catalyst can work under visible light conditions. Therefore, the alkylation of aldehydes with this amino-photocatalyst works with excellent enantioselectivities and yields due to the stereoelectronic properties of the catalyst. Laser flash photolysis experiments showed that the intramolecular quenching of the excited state (singlet or triplet) of the thioxanthone moiety by the amino group in the bifunctional catalyst is reduced after the enamine formation. In addition, we have found that the bifunctional catalyst **4c** possesses a lower quantum yield compared to other previous photo-catalytic systems which can be attributed to the contribution of the internal redox process. Moreover, ground state geometry optimization and energy transition studies of thioxanthone and the bifunctional catalyst **4c** were optimized by TD DFT calculations. A rational mechanistic cycle based on different mechanistic experiments, TD DFT calculations, and laser flash photolysis has also been presented.

ASSOCIATED CONTENT

Supporting Information.

The following files are available free of charge.

Experimental details, general procedures, optimization of reaction conditions, characterization of

products, copies of NMR and HPLC spectra of all products, fluorescence studies, computational details and theoretical results (PDF).

AUTHOR INFORMATION

Corresponding Author

* Departamento de Química Orgánica (Módulo 1), Facultad de Ciencias, Universidad Autónoma de Madrid, 28049-Madrid, Spain. E-mail: jose.aleman@uam.es

Author Contributions

All authors have given approval to the final version of the manuscript.

ACKNOWLEDGMENT

Spanish Government (CTQ2015-64561-R) and the European Research Council (ERC-CG, contract number: 647550) are acknowledged. We acknowledge the generous allocation of computing time at the CCC (UAM).

REFERENCES

(1) For recent selected reviews, see: (a) Prier, C. K.; Rankic, D. A.; MacMillan, D. W. C. *Chem Rev*. **2013**, *113*, 5322-5363. (b) Skubi, K. L.; Blum, T. R.; Yoon, T. P. *Chem. Rev.* **2016**, *116*, 10035–10074. (c) Pitre, S. P.; McTiernan, C. D.; Scaiano, J. C. *ACS Omega* **2016**, *1*, 66–76. (d) Romero N. A.; Nicewicz, D. A. *Chem. Rev.* **2016**, *116*, 10075–10166. (e) Narayanam, J. M. R.; Stephenson, C. R. J. *Chem. Soc. Rev*., **2011**, *40*, 102-113. (f) Ravelli, D.; Protti, S.; Fagoni, M. *Chem. Rev.* **2016**, *116*, 9850-9913.

(2) Curran, D. P.; Porter, N. A.; Giese, B. *Stereochemistry of Radical Reactions: Concepts, Guidelines, and Synthetic Applications*, VCH 1996.

(3) For pioneering examples in cooperative asymmetric photo-organocatalytic systems, see: (a) Nicewicz, D. A.; MacMillan, D. W. C. *Science* **2008**, *322*, 77-80. (b) Nagib, D. A.; Scott, M. E.; MacMillan, D. W. C. *J. Am. Chem. Soc.* **2009**, *131*, 10875–10877. (c) Shih, H.-W.; Wal, M. N. V.; Grange, R. L.; MacMillan, D. W. C. *J. Am. Chem. Soc.* **2010**, *132*, 13600-13603. (d) Welin, E. R.; Warkentin, A. A.; Conrad, J. C.; MacMillan, D. W. C. *Angew. Chem. Int. Ed.* **2015**, *54*, 9668 –9672. (e) Capacci, A. G.; Malinowski, J. T.; McAlpine, N. J.; Kuhne, J.; MacMillan, D. W. C. *Nature Chem.* **2017**, *9*, 1073-1077.

(4) Bauer, A.; Westkamper, F.; Grimme, S. Bach, T. *Nature*, **2005**, *436*, 1139-1140.

(5) Ding, W.; Lu, L.-Q.; Zhou, Q.-Q.; Wei, Y.; Chen, J.-R.; Xiao, W.-J. *J. Am. Chem. Soc.* **2017**, *139*, 63-66.

(6) (a) Huo, H.; Shen, X.; Wang, C. Zhang, L.; Rose, P.; Chen, L.-A.; Harms, K.; Marsch, M.; Hilt, G. Meggers, E. *Nature*, **2014**, *515*, 100-103. (b) Ma, J.; Rosales, A. R.; Huang, X; Harms, K.; Riedel, R.; Wiest, Olaf.; Meggers, E. *J. Am. Chem. Soc.* **2017**, *139*, 17245–17248. (c) Meggers, E. *Angew. Chem. Int. Ed.* **2017**, *56*, 5668-5675, and references cited therein.

(7) For a review on enantioselective photofunctionalization of aldehydes and ketones see: Zou, Y.-Q.; Hörmann, F. M.; Bach, T. *Chem. Soc. Rev.* **2018**, DOI: 10.1039/C7CS00509.

(8) Gualandi, A.; Marchini, M.; Mengozzi, L.; Natali, M.; Lucarini, M.; Ceroni, P.; Cozzi, P. G. *ACS Catal.* **2015**, *5*, 5927-5931.

(9) (a) Riente, P.; Matas Adams, M.; Albero, J.; Palomares, E.; Pericàs, M. A. *Angew. Chem. Int. Ed.* **2014**, *53*, 9613-9616. (b) Cherevatskaya, M.; Neumann, M.; Füldner, S.;

Harlander, C.; Kümmel, S.; Dankesreiter, S.; Pfitzner, A.; Zeitler, K.; König, B. *Angew. Chem. Int. Ed.* **2012**, *51*, 4032-4066.

(10) Neumann, M.; Füldner, S.; König, B.; Zeitler, K. *Angew. Chem. Int. Ed.* **2011**, *50*, 951-954.

(11) Fidaly, K.; Ceballos, C.; Falguières, A.; Sylla-Iyarreta Veitia, M.; Guy, A.; Ferroud, C. *Green Chem.* **2012**, *14*, 1293-1297.

(12) For some contribution of our groups in the field of the bifunctional organocatalysts, see: (a) C. Jarava-Barrera, F. Esteban, C. Navarro-Ranninger, A. Parra and J. Alemán, *Chem. Commun.* 2013, **49**, 2001. (b) A. Parra, R. Alfaro, L. Marzo, A. Moreno-Carrasco, J. L. García Ruano and J. Alemán, *Chem. Commun* 2012, **48**, 9759. (c) V. Marcos, J. Alemán, J. L. García Ruano, F. Marini, T. Marcello *Org. Lett.* 2011, **13**, 3052. (d) M. Frías, R. Mas-Balleste, S. Arias, C. Alvarado and J. Alemán *J. Am. Chem. Soc*. 2017, **139**, 672-679. (e) Frias, M.; Carrasco, A. C.; Fraile, A.; Alemán, J. *Chem. Eur. J.* **2018**, DOI: 10.1002/chem.201705218. (f) Esteban, F.; Cieślik, W.; Arpa, E. M.; Guerrero-Corella, A.; Díaz-Tendero, S.; Perles, J.; Fernández-Salas, J. A.; Fraile, A.; Alemán, J. *ACS Catal* **2018**, *8*, 1884–1890.

(13) Dadashi-Silab, S.; Aydogan, C.; Yagci, Y. *Polym. Chem.* **2015**, *6*, 6595-6615.

(14) (a) Ding, W.; Lu, L.-Q.; Zhou, Q.-Q.; Wei, Y.; Chen, J.-R.; Xiao, W.-J. *J. Am. Chem. Soc.* **2017**, *139*, 63-66. (b) Tripathi, C. B.; Ohtani, T.; Corbett, M. T.; Ooi, T. *Chem. Sci.* **2017**, *8*, 5622-5627.

(15) For selected examples see: (a) Tröster, A.; Alonso, R.; Bauer, A.; Bach, T. *J. Am. Chem. Soc.* **2016**, *138*, 7808-7811. (b) Mayr, F.; Brimioulle, R.; Bach, T. *J. Org. Chem.* **2016**, *81*, 6965–6971. (c) Alonso, R.; Bach, T. *Angew. Chem. Int. Ed.* **2014**, *53*, 4368-4371.

(16) Neumann, M. G.; Gehlen, M. H.; Encinas, M. V.; Allen, N. S.; Corrales, T.; Peinado, C.; Catalina, F. *J. Chem. Soc., Faraday Trans.* **1997**, *93*, 1517-1521.

(17) (a) Wöll, D.; Smirnova, J.; Galetskaya, M.; Prykota, T.; Bühler, J.; Stengele, K.-P.; Pfleiderer, W.; Steiner, U. E. *Chem. Eur. J.* **2008**, *14*, 6490-6497. (b) Harwood, J. S.; Marynick, D. S.; Ternay, A. L. Jr., *J. Chem. Soc., Perkin Trans. 2: Phys. Org. Chem.* **1989**, *4*, 325-330.

(18) CCDC 1819092 and CCDC 1819093 contains the crystallographic data of compounds 4b and 4c, respectively. These data can be obtained free of charge from The Cambridge Crystallographic Data Centre via www.ccdc.cam.ac.uk/data_request/cif.

(19) R. Mundt, T. Villnow, Ch. Torres Ziegenbein, P. Gilch, Ch. Marian V. Rai-Constapel, Phys. Chem. Chem. Phys., 2016, 18, 6637-6647,

(20) V. Rai-Constapel, T. Villnow, G. Ryseck, P. Gilch and C. M. Marian, J. Phys. Chem. A, 2014, 11708–11717

(21) Ò. Rubio-Pons, L. Serrano-Andrés, D. Burget and P. Jacques, J. Photochem. Photobiol., A, 2006, 179, 298–304

(22) V. Rai-Constapel, M. Kleinschmidt, S. Salzmann, L. Serrano-Andres Ch.M. Marian Phys. Chem. Chem. Phys., 2010, 12, 9320-9327.

(23) S. Ishijima, M. Higashi and H. Yamaguchi, J. Phys. Chem., 1994, 98, 10432–10435

(24) Herkstroeter WG, Lamola AA, Hammokd GS. Mechanisms of photochemical reactions in solution XXVIII. Values of triplet excitation energies of selected sensitizers. J. Am. Chem. Soc. 1964;86:4537–4540.

(25) For EDA complexes, see: (a) Arceo, E.; Jurberg, I. D.; Álvarez-Fernández, A.; Melchiorre, P. *Nature Chem*. **2013**, 5, 750-756. (b)

(26) For the visible light absorption of the enamine, see: (a) Silvi, M.; Arceo, E.; Jurberg, I. D. Cassani, C.; Melchiorre, P. *J. Am. Chem. Soc.* **2015**, *137*, 6120-6123.

(27) For a completed studied in the alkylation of enamines with the Jorgensen-Hayashi catalyst, see: Bahamonde, A.; Melchiorre, P. *J. Am. Chem. Soc*. **2016**, *138*, 8019-8030.

(28) We have tried several conditions for the synthesis of En-4c in all the cases with unfruitful results.

(29) Cismesia, M. A.; Yoon, T. P. *Chem. Sci.* **2015**, *6*, 5426-5434.

(30) Kuhn, H. J.; Braslavsky, S. E.; Schmidt, R. *Pure Appl. Chem.* **2004**, *76*, 2105–2146.

(31) In order to determine the thermodynamic feasibility of radical-chain pathways in our photocatalytic system, DFT calculations of **En-4c** were performed (propagation step, Scheme 5). Oxidation of the resultant radical intermediate (intermediate **III**, Scheme 5) occurs by an exergonic process, leading to an enamine cation (intermediate **IV**, Scheme 5). See S.I. for further details.

(32) Karasu, F.; Arsu, N.; Jockusch, S.; Turro, N. J. *Macomolecules*, **2009**, *42*, 7318.

Graphical Abstract: